

The gravitational potential at fifth order

Andreas Maier

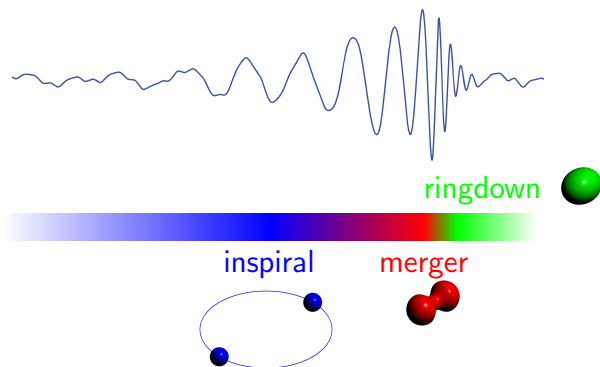


20 May 2021

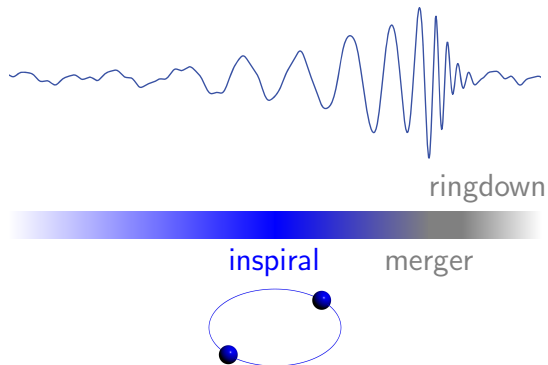
In collaboration with

Johannes Blümlein Peter Marquard Gerhard Schäfer

Gravitational waves from binary mergers

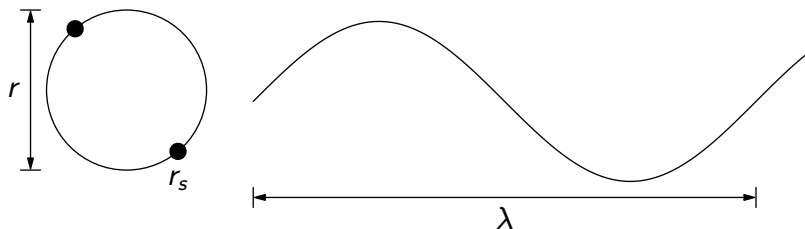


Gravitational waves from binary mergers



Compact binary systems

Post-Newtonian expansion



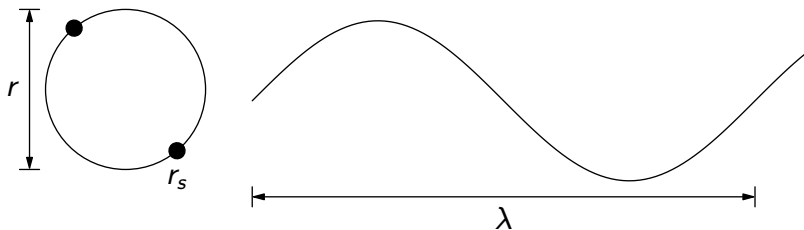
- Masses comparable: $m \equiv m_1 \sim m_2$
Generalisation to different masses straightforward
- Nonrelativistic system: $v \ll 1$
- Virial theorem: $mv^2 \sim \frac{Gm^2}{r}$

Post-Newtonian (PN) expansion:
Combined expansion in $v \sim \sqrt{Gm/r} \ll 1$

Alternative: Post-Minkowskian expansion \Rightarrow Mao Zeng's talk

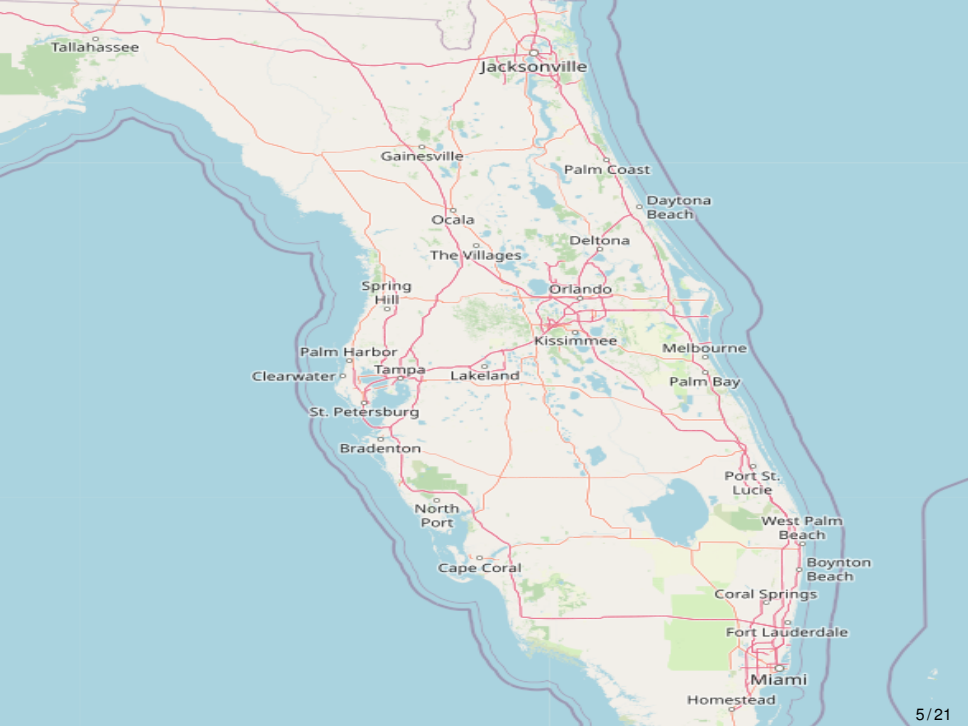
Post-Newtonian expansion

Scales



- $\omega_{\text{GW}} = \frac{2v}{r} \Rightarrow \lambda \sim \frac{r}{v}$

- $r_s = 2Gm \Rightarrow r_s \sim rv^2$



Tallahassee

Jacksonville

Gainesville

Palm Coast

Daytona Beach

Ocala

Deltona

The Villages

Spring Hill

Orlando

Palm Harbor

Kissimmee

Melbourne

Clearwater

Tampa

Lakeland

Palm Bay

St. Petersburg

Bradenton

Port St. Lucie

North Port

West Palm Beach

Cape Coral

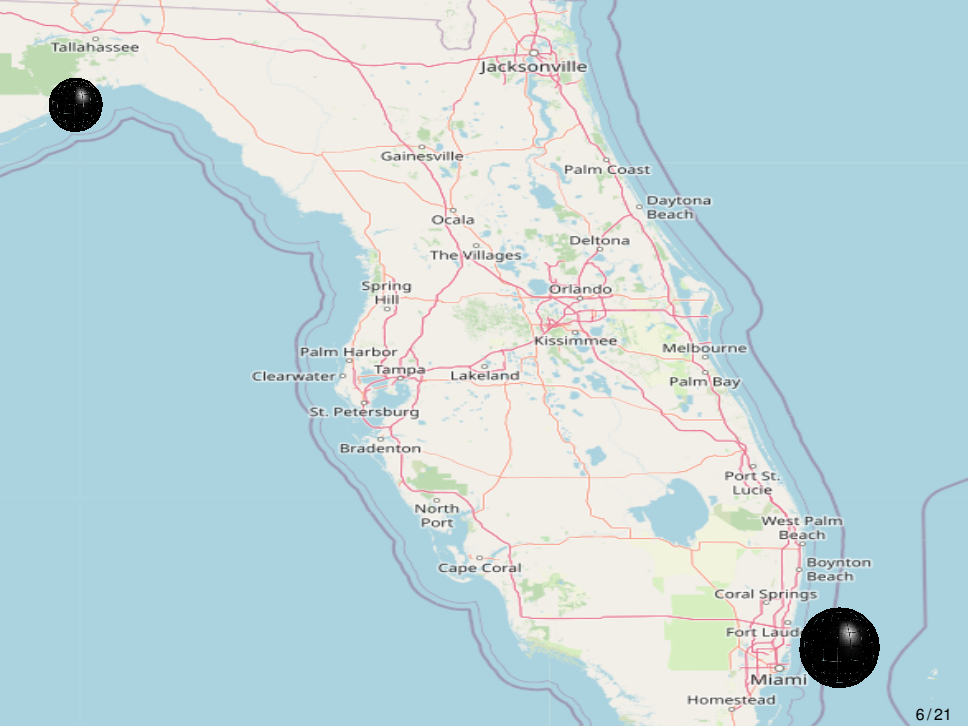
Boynton Beach

Coral Springs

Fort Lauderdale

Miami

Homestead



Central quantities

Energy and flux

- Emission of quadrupole waves: $\omega_{\text{GW}}(t) = 2\omega(t)$
- Orbital frequency ω from continuity equation:

$$\frac{dE(\omega)}{dt} = -F(\omega) \quad \Rightarrow \quad \dot{\omega}(t) = -\frac{F(\omega)}{dE(\omega)/d\omega}$$

E : Centre-of-mass energy

F : Gravitational wave luminosity

$$\dot{\omega}_{\text{GW}}(t) = -2\frac{F(\omega)}{dE(\omega)/d\omega}$$

Determine $F(\omega)$, $E(\omega)$ from a [Post-Newtonian Lagrangian](#)

Effective Field Theory

Idea: construct simpler, but equivalent theory

Starting from a full theory (general relativity)

- 1 Identify relevant **scales** and expand action in **small scaling parameter**

$$v \sim \sqrt{Gm/r} \ll 1$$

General relativity

Post-Newtonian expansion

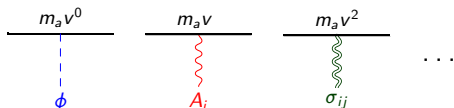
Temporal Kaluza-Klein decomposition [Kol, Smolkin 2010]

$$g^{\mu\nu} = e^{2\phi} \begin{pmatrix} -1 & A_j \\ A_i & e^{-c_d\phi}(\delta_{ij} + \sigma_{ij}) - A_i A_j \end{pmatrix}, \quad c_d = 2 \frac{d-2}{d-3}$$

Post-Newtonian expansion in $\phi, A_i, \sigma_{ij} \sim v \sim \sqrt{Gm/r} \ll 1$:

$$S_{\text{GR}}[\phi, A_i, \sigma_{ij}] =$$

$$\begin{aligned} & \sum_{a=1}^2 \int dt \left(m_a + \frac{1}{2} m_a v_a^2 + \mathcal{O}(v^4) \right) \\ & + \sum_{a=1}^2 m_a \int dt \left(-\phi + v_{ai} A_i + v_{ai} v_{aj} \sigma_{ij} - \frac{1}{2} \phi^2 + \dots \right) \\ & + \int \frac{d^d x}{32\pi G} \left[-c_d (\partial_\mu \phi)^2 + (\partial_\mu A_i)^2 + \frac{1}{4} (\partial_\mu \sigma_{ij})^2 - \frac{1}{2} (\partial_\mu \sigma_{ij})^2 + \dots \right] \end{aligned}$$



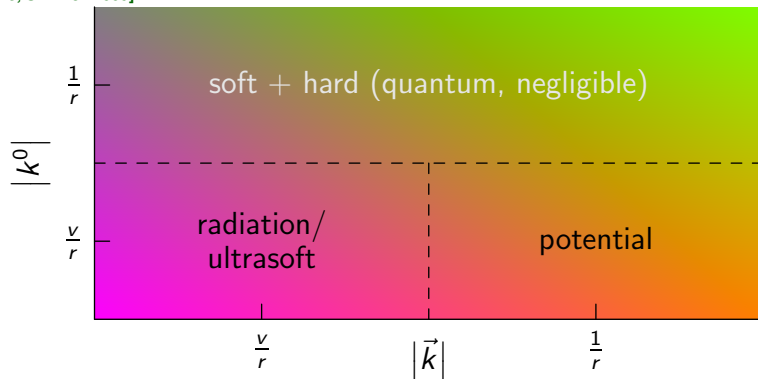
Effective field theory

Starting from a full theory (general relativity)

- 1 Identify relevant scales and expand action in small scaling parameter
- 2 Decompose fields into **modes**, characterised by scaling of momentum components

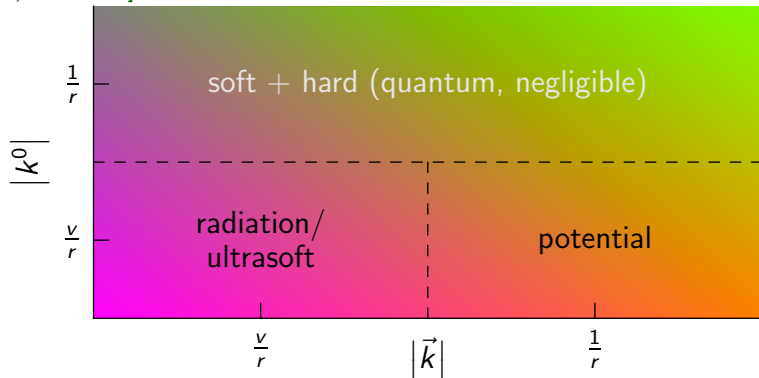
Decomposition into field modes

[Beneke, Smirnov 1999]



Decomposition into field modes

[Beneke, Smirnov 1999]

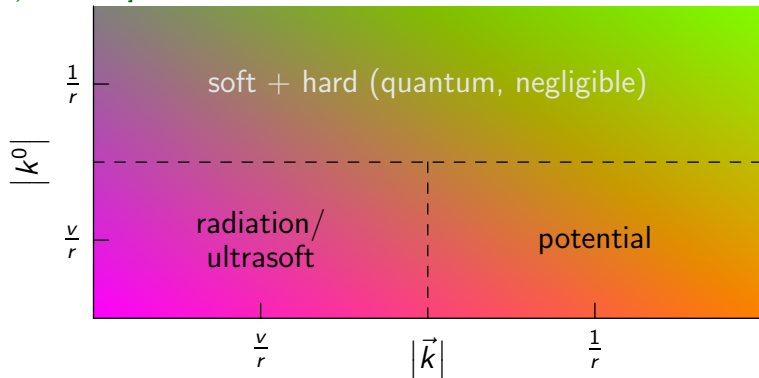


$$\int_{\mathbb{R}^d} dk I = \int_{\text{rad}} dk T_{\text{rad}} I + \int_{\text{pot}} dk T_{\text{pot}} I = \int_{\mathbb{R}^d} dk T_{\text{pot}} I + \int_{\mathbb{R}^d} dk T_{\text{rad}} I$$

$T_{\text{pot/rad}}$: expansion according to potential/radiation scaling

Decomposition into field modes

[Beneke, Smirnov 1999]



$$\int_{\mathbb{R}^d} dk I = \int_{\text{rad}} dk T_{\text{rad}} I + \int_{\text{pot}} dk T_{\text{pot}} I = \int_{\mathbb{R}^d} dk T_{\text{pot}} I + \int_{\mathbb{R}^d} dk T_{\text{rad}} I$$

$T_{\text{pot/rad}}$: expansion according to potential/radiation scaling

Equivalently: $\phi = \phi_{\text{rad}} + \phi_{\text{pot}}$, $A = A_{\text{rad}} + A_{\text{pot}}$, $\sigma = \sigma_{\text{rad}} + \sigma_{\text{pot}}$

Effective Field Theory

Starting from a full theory (general relativity)

- 1 Identify relevant scales and expand action in small scaling parameter
- 2 Decompose fields into modes, characterised by scaling of momentum (components)
- 3 Write down effective field theory action:
Nonrelativistic general relativity [Goldberger, Rothstein 2004-2006]

- Absorb **potential modes** into **near-zone potential**
- Keep **radiation/ultrasoft modes**

Ansatz:

$$S_{\text{NRGR}} = S_{\text{matter}} + S_{\text{mixed}} + S_{\text{radiation}}$$

- $S_{\text{matter}} = \int dt (M + T - V_{\text{NZ}})$
- S_{mixed} : coupling of radiation modes to matter
- $S_{\text{radiation}}$: pure radiation modes

Effective Field Theory

Starting from a full theory (general relativity)

- 1 Identify relevant scales and expand action in small scaling parameter
- 2 Decompose fields into modes, characterised by scaling of momentum (components)
- 3 Write down effective field theory action
- 4 Determine parameters from **equivalence** between effective and full theory up to higher PN orders: **matching**

Nonrelativistic effective theory

Potential matching

$$V_{\text{NZ}} = i \frac{d}{dt} \log \left[\int \mathcal{D}\phi_{\text{pot}} \mathcal{D}A_{\text{pot}} \mathcal{D}\sigma_{\text{pot}} e^{iS_{\text{GR}} - i \int dt (M+T)} \Big|_{\phi_{\text{rad}}=A_{\text{rad}}=\sigma_{\text{rad}}=0} \right]$$
$$= i \frac{d}{dt} \log \left[1 + \text{---} \text{---} + \text{---} \text{---} + \frac{1}{2} \times \text{---} \text{---} + \frac{1}{2} \times \text{---} \text{---} + \dots \right]$$

Matter lines are no propagators:

$$\text{---} \text{---} = \begin{array}{c} \circ \\ | \\ \circ \end{array} \begin{array}{c} \circ \\ | \\ \circ \end{array} = \left(\text{---} \text{---} \right)^2$$

No contributions from factorising diagrams:

cf. [Fischler 1977]

$$V_{\text{NZ}} = i \frac{d}{dt} \left[\text{---} \text{---} + \text{---} \text{---} + \frac{1}{2} \times \text{---} \text{---} + \dots \right]$$

Potential matching

5PN calculation

- 1 Generate diagrams with up to 5 loops with QGRAF [Nogueira 1991]
- 2 Discard unwanted diagrams, e.g. graviton loops

$$-i \int dt V_{5\text{PN}} =$$

The diagram illustrates the generation of Feynman diagrams for the 5PN potential. It shows a series of diagrams arranged in three rows and four columns, separated by plus signs. Each diagram consists of two horizontal black lines representing worldlines. Blue dashed lines represent graviton exchanges between the worldlines. Green wavy lines represent ghost loops. The diagrams show increasing complexity from top-left to bottom-right, with the last diagram in the third row followed by an ellipsis. The first row contains four diagrams with 1, 2, 3, and 4 graviton exchanges. The second row contains four diagrams with 2, 3, 4, and 5 graviton exchanges. The third row contains three diagrams with 3, 4, and 5 graviton exchanges, followed by an ellipsis.

Potential matching

5PN calculation

- 1 Generate diagrams with up to 5 loops with QGRAF [Nogueira 1991]
- 2 Discard unwanted diagrams, e.g. graviton loops
- 3 Compute and insert Feynman rules with FORM [Vermaseren et al.]

$$\begin{array}{c} i_1 i_2 \\ p_1 \\ \text{---} \\ p_2 \\ \text{---} \\ j_1 j_2 \end{array} \begin{array}{c} k_1 k_2 \\ \text{---} \\ \text{---} \\ \text{---} \end{array} = \frac{i}{32\pi^2} (\tilde{V}_{\sigma\sigma\sigma}^{i_1 i_2 j_1 j_2, k_1 k_2} + \tilde{V}_{\sigma\sigma\sigma}^{i_2 i_1 j_1 j_2, k_1 k_2})$$

$$\begin{aligned}
 \tilde{V}_{\sigma\sigma\sigma}^{i_1 i_2 j_1 j_2, k_1 k_2} &= V_{\sigma\sigma\sigma}^{i_1 i_2 j_1 j_2, k_1 k_2} + V_{\sigma\sigma\sigma}^{i_1 i_2 j_2 j_1, k_1 k_2} + V_{\sigma\sigma\sigma}^{i_1 i_2 j_1 j_2, k_2 k_1} + V_{\sigma\sigma\sigma}^{i_1 i_2 j_2 j_1, k_2 k_1} \\
 V_{\sigma\sigma\sigma}^{i_1 i_2 j_1 j_2, k_1 k_2} &\stackrel{\nu=0}{=} (\vec{p}_1^2 + \vec{p}_1 \cdot \vec{p}_2 + \vec{p}_2^2) \left(-\delta^{j_1 j_2} (2\delta^{i_1 k_1} \delta^{i_2 k_2} - \delta^{i_1 i_2} \delta^{k_1 k_2}) \right. \\
 &\quad \left. + 2[\delta^{i_1 j_1} (4\delta^{i_2 k_1} \delta^{j_2 k_2} - \delta^{i_2 j_2} \delta^{k_1 k_2}) - \delta^{i_1 i_2} \delta^{j_1 k_1} \delta^{j_2 k_2}] \right) \\
 &\quad + 2\left\{ 4(p_1^{k_2} p_2^{j_2} - p_1^{j_2} p_2^{k_2}) \delta^{i_1 j_1} \delta^{j_2 k_1} \right. \\
 &\quad \left. + 2[(p_1^{i_1} + p_2^{i_1}) p_2^{j_2} \delta^{j_1 k_1} \delta^{j_2 k_2} - p_1^{k_1} p_2^{k_2} \delta^{i_1 j_1} \delta^{i_2 j_2}] \right. \\
 &\quad \left. + \delta^{j_1 j_2} [p_1^{k_1} p_2^{k_2} \delta^{i_1 i_2} + 2(p_1^{k_2} p_2^{j_2} - p_1^{j_2} p_2^{k_2}) \delta^{i_1 k_1} - (p_1^{i_1} + p_2^{i_1}) p_2^{j_2} \delta^{k_1 k_2}] \right. \\
 &\quad \left. + p_2^{j_2} (4p_1^{j_2} \delta^{i_1 k_1} \delta^{j_1 k_2} + p_1^{j_1} (2\delta^{i_1 k_1} \delta^{i_2 k_2} - \delta^{i_1 i_2} \delta^{k_1 k_2})) \right. \\
 &\quad \left. + 2[\delta^{i_1 j_1} (p_1^{j_2} \delta^{k_1 k_2} - 2p_1^{k_2} \delta^{i_2 k_1}) - p_1^{k_2} \delta^{i_1 i_2} \delta^{j_1 k_1}] \right) \\
 &\quad \left. + p_1^{j_2} (p_1^{j_1} (2\delta^{i_1 k_1} \delta^{i_2 k_2} - \delta^{i_1 i_2} \delta^{k_1 k_2}) - 4p_2^{j_2} \delta^{i_1 k_1} \delta^{j_1 k_2} \right. \\
 &\quad \left. + 2[p_2^{k_2} \delta^{i_1 i_2} \delta^{j_1 k_1} + \delta^{i_1 j_1} (2p_2^{k_2} \delta^{i_2 k_1} - p_2^{j_2} \delta^{k_1 k_2})] \right) \left. \right\}
 \end{aligned}$$

Potential matching

5PN calculation

- 1 Generate diagrams with up to 5 loops with QGRAF [Nogueira 1991]
- 2 Discard unwanted diagrams, e.g. graviton loops
- 3 Compute and insert Feynman rules with FORM [Vermaseren et al.]
- 4 Reduce massless propagators to master integrals using Laporta's algorithm [Chetyrkin, Tkachov 1981, Laporta 2000] implemented in `crusher`

$$V_{\text{NZ}}^{5\text{PN}} \stackrel{v=0}{=} c_0 \text{ (diagram)} + c_1 \text{ (diagram)} + c_2 \text{ (diagram)} + c_3 \text{ (diagram)} + \mathcal{O}(\epsilon)$$

c_j : Laurent series in $\epsilon = \frac{3-d}{2}$,
polynomials in m_1, m_2, r^{-1}, G^{-1}

Potential matching

5PN calculation

- 1 Generate diagrams with up to 5 loops with QGRAF [Nogueira 1991]
- 2 Discard unwanted diagrams, e.g. graviton loops
- 3 Compute and insert Feynman rules with FORM [Vermaseren et al.]
- 4 Reduce massless propagators to master integrals using Laporta's algorithm [Chetyrkin, Tkachov 1981, Laporta 2000] implemented in `crusher`
- 5 Insert known (factorising) master integrals
[Lee, Mingulov 2015; Damour, Jaranowski 2017]

$$\text{Diagram} = 6\pi^{7/2} \left[\frac{2}{\epsilon} - 4 - 4 \ln(2) + \mathcal{O}(\epsilon^1) \right]$$

Potential matching

5PN calculation

- 1 Generate diagrams with up to 5 loops with QGRAF [Nogueira 1991]
- 2 Discard unwanted diagrams, e.g. graviton loops
- 3 Compute and insert Feynman rules with FORM [Vermaseren et al.]
- 4 Reduce massless propagators to master integrals using Laporta's algorithm [Chetyrkin, Tkachov 1981, Laporta 2000] implemented in `crusher`
- 5 Insert known (factorising) master integrals

[Lee, Mingulov 2015; Damour, Jaranowski 2017]

$$V_{5PN}^{NZ} \stackrel{v \ll 0}{\equiv} \frac{G^6}{r^6} m_1 m_2 \left[\frac{5}{16} (m_1^5 + m_2^5) + \frac{91}{6} m_1 m_2 (m_1^3 + m_2^3) + \frac{653}{6} m_1^2 m_2^2 (m_1 + m_2) \right]$$

5PN $v = 0$: [Foffa, Mastrolia, Sturani, Sturm, Torres Bobadilla 2019; Blümlein, Maier, Marquard 2019]

New:

- complete 5PN [Blümlein, Maier, Marquard, Schäfer, 2020]
partial 5PN (parts of $v^2 G^5$) [Foffa, Sturani, Torres Bobadilla 2020]
- 6PN up to 3 loops: $v \geq 6$ [Blümlein, Maier, Marquard, Schäfer, 2020-2021]

Classical action

V_{NZ} is not physical:

- Gauge dependent
- Infrared divergence at $\geq 4\text{PN}$

\Rightarrow combine with contribution from radiation/ultrasoft modes

Classical action

V_{NZ} is not physical:

- Gauge dependent
- Infrared divergence at $\geq 4\text{PN}$

\Rightarrow combine with contribution from radiation/ultrasoft modes

Construct classical post-Newtonian action *without* any field:

$$S_{\text{PN}} = \int dt L[\vec{x}_a, \vec{v}_a] = \int dt (M + T - V)$$

Absorb radiation modes radiation/ultrasoft modes into far-zone potential V_{FZ} (“tail”)

$$V = V_{\text{NZ}} + V_{\text{FZ}}$$

$V_{\text{FZ}}^{5\text{PN}}$ from combination of known results

[Ross 2012] [Marchand, Henry, Larrouturou, Marsat, Faye, Blanchet 2020] [Foffa, Sturani 2019–2021]

Classical Hamiltonian

$$\mu = \frac{m_1 m_2}{M}, \quad p = \frac{\vec{p}_1}{\mu} = -\frac{\vec{p}_2}{\mu}, \quad r = \frac{|x_1 - x_2|}{GM}, \quad n = \frac{\vec{r}}{r}$$

$$\begin{aligned} \frac{H_{5PN}^{\text{pole free}} - M}{\mu} = & -\frac{21p^{12}}{1024} + \frac{5}{16r^6} - \frac{125p^2}{16r^5} - \frac{499p^4}{64r^4} - \frac{161p^6}{32r^3} - \frac{445p^8}{256r^2} - \frac{77p^{10}}{256r} \\ & + \frac{\mu}{M} \left[\frac{231p^{12}}{1024} - \frac{279775133}{529200r^6} - \frac{1450584679p^2}{2116800r^5} + \frac{2010713771p^4}{1411200r^4} + \frac{11206267p^6}{141120r^3} + \frac{937p^8}{32r^2} \right. \\ & + \frac{805p^{10}}{256r} + \ln\left(\frac{r}{r_0}\right) \left(\frac{64}{105r^6} - \frac{18944p^2}{105r^5} + \frac{1796p^4}{105r^4} + \frac{19136(p.n)^2}{105r^5} - \frac{10664p^2(p.n)^2}{105r^4} \right. \\ & + \left. \frac{2748(p.n)^4}{35r^4} \right) + \pi^2 \left(\frac{70399}{1152r^6} + \frac{65291p^2}{1152r^5} - \frac{1328147p^4}{12288r^4} - \frac{7719p^6}{4096r^3} + \frac{6649(p.n)^2}{576r^5} \right. \\ & + \frac{5042575p^2(p.n)^2}{6144r^4} + \frac{58887p^4(p.n)^2}{4096r^3} - \frac{3293913(p.n)^4}{4096r^4} - \frac{89625p^2(p.n)^4}{4096r^3} \\ & + \left. \frac{42105(p.n)^6}{4096r^3} \right) - \frac{34541593(p.n)^2}{2116800r^5} - \frac{2395722563p^2(p.n)^2}{282240r^4} - \frac{62196341p^4(p.n)^2}{78400r^3} \\ & - \frac{589p^6(p.n)^2}{16r^2} - \frac{35p^8(p.n)^2}{256r} + \frac{631107353(p.n)^4}{78400r^4} + \frac{31226291p^2(p.n)^4}{23520r^3} \\ & + \frac{8951p^4(p.n)^4}{384r^2} - \frac{563921(p.n)^6}{960r^3} - \frac{5117p^2(p.n)^6}{320r^2} + \frac{159(p.n)^8}{28r^2} \left. \right] + \frac{\mu^2}{M^2} \left[-\frac{231p^{12}}{256} \right. \\ & + \frac{72454}{225r^6} + \frac{1353196483p^2}{529200r^5} - \frac{787300061p^4}{264600r^4} + \frac{3605263p^6}{29400r^3} - \frac{11535p^8}{128r^2} - \frac{2865p^{10}}{256r} \\ & \left. - \ln\left(\frac{r}{r_0}\right) \left(\frac{256}{105r^6} + \frac{3392p^2}{105r^5} - \frac{432p^4}{35r^4} - \frac{2992(p.n)^2}{105r^5} - \frac{6824p^2(p.n)^2}{105r^4} + \frac{496(p.n)^4}{7r^4} \right) \right] \end{aligned}$$

Classical Hamiltonian

$$\begin{aligned}
 & + \pi^2 \left(\frac{5453}{768r^6} - \frac{121315p^2}{768r^5} + \frac{2076041p^4}{12288r^4} + \frac{29987p^6}{4096r^3} + \frac{200359(p.n)^2}{768r^5} - \frac{172311p^4(p.n)^2}{4096r^3} \right. \\
 & - \frac{5962205p^2(p.n)^2}{6144r^4} + \frac{2617363(p.n)^4}{4096r^4} + \frac{127125p^2(p.n)^4}{4096r^3} + \frac{14175(p.n)^6}{4096r^3} \left. \right) \\
 & - \frac{857318207(p.n)^2}{264600r^5} + \frac{34200172759p^2(p.n)^2}{2116800r^4} - \frac{5034763p^4(p.n)^2}{9800r^3} + \frac{4969p^6(p.n)^2}{64r^2} \\
 & + \frac{275p^8(p.n)^2}{256r} - \frac{4989943687(p.n)^4}{352800r^4} + \frac{2674877p^2(p.n)^4}{7840r^3} + \frac{925p^4(p.n)^4}{24r^2} + \frac{15p^6(p.n)^4}{128r} \\
 & - \frac{25649(p.n)^6}{3360r^3} - \frac{8331p^2(p.n)^6}{160r^2} + \frac{751(p.n)^8}{28r^2} \left. \right] + \frac{\mu^3}{M^3} \left[\frac{1617p^{12}}{1024} - \frac{238966727p^2}{151200r^5} \right. \\
 & + \frac{127702733p^4}{84672r^4} + \frac{108551131p^6}{4233600r^3} + \frac{16283p^8}{256r^2} + \frac{3995p^{10}}{256r} + \pi^2 \left(-\frac{2339p^2}{192r^5} + \frac{98447p^4}{3072r^4} \right. \\
 & - \frac{20259p^6}{1024r^3} - \frac{16111(p.n)^2}{192r^5} + \frac{131231p^2(p.n)^2}{1536r^4} + \frac{106947p^4(p.n)^2}{1024r^3} - \frac{361499(p.n)^4}{1024r^4} \\
 & - \left. \frac{30075p^2(p.n)^4}{1024r^3} - \frac{65625(p.n)^6}{1024r^3} \right) + \frac{758233181(p.n)^2}{151200r^5} - \frac{10374288811p^2(p.n)^2}{705600r^4} \\
 & - \frac{2207947669p^4(p.n)^2}{1411200r^3} + \frac{177p^6(p.n)^2}{256r^2} - \frac{221p^8(p.n)^2}{64r} + \frac{12810612439(p.n)^4}{705600r^4} \\
 & + \frac{355111837p^2(p.n)^4}{94080r^3} - \frac{125225p^4(p.n)^4}{768r^2} - \frac{3p^6(p.n)^4}{128r} - \frac{13905527(p.n)^6}{4480r^3} \\
 & \left. + \frac{136977p^2(p.n)^6}{1280r^2} - \frac{15p^4(p.n)^6}{128r} - \frac{289839(p.n)^8}{4480r^2} - \frac{35p^2(p.n)^8}{256r} \right]
 \end{aligned}$$

Classical Hamiltonian

$$\begin{aligned}
 & + \frac{\mu^4}{M^4} \left[-\frac{1155p^{12}}{1024} - \frac{593p^6}{32r^3} + \frac{6649p^8}{256r^2} - \frac{1615p^{10}}{256r} + \frac{549p^4(p.n)^2}{32r^3} - \frac{62143p^6(p.n)^2}{256r^2} + \frac{867p^8(p.n)^2}{256r} \right. \\
 & - \frac{5749p^2(p.n)^4}{96r^3} + \frac{652381p^4(p.n)^4}{768r^2} - \frac{3p^6(p.n)^4}{64r} - \frac{17623(p.n)^6}{240r^3} - \frac{1178329p^2(p.n)^6}{1280r^2} \\
 & \left. - \frac{45p^4(p.n)^6}{128r} + \frac{1443091(p.n)^8}{4480r^2} + \frac{105p^2(p.n)^8}{128r} \right] + \frac{\mu^5}{M^5} \left[\frac{231p^{12}}{1024} - \frac{63p^{10}}{256r} - \frac{35p^8(p.n)^2}{256r} \right. \\
 & \left. - \frac{15p^6(p.n)^4}{128r} - \frac{15p^4(p.n)^6}{128r} - \frac{35p^2(p.n)^8}{256r} - \frac{63(p.n)^{10}}{256r} \right] + \frac{17(p.n)^2}{4r^5} + \frac{29p^2(p.n)^2}{8r^4} \\
 & + \frac{21p^4(p.n)^2}{16r^3} + \frac{5p^6(p.n)^2}{32r^2} - \frac{(p.n)^4}{8r^4} + V_{\text{FZ,fin, non-log}}^{\text{SPN}}
 \end{aligned}$$

⇒ observables: energy, periastron advance

Classical Hamiltonian

Cross checks:

- ✓ $\frac{\mu^0}{M^0}$ agrees with Schwarzschild limit
- ✓ $\frac{\mu^1}{M^1}, \frac{\mu^2}{M^2}$: poles cancel between **near zone** and **far zone**
- ✓ $\frac{\mu^3}{M^3}, \frac{\mu^4}{M^4}, \frac{\mu^5}{M^5}$ agree with [Bini, Damour, Geralico 2020]
- $\frac{\mu^1}{M^1}$ agrees with [Bini, Damour, Geralico 2020]
after finite renormalisation of gravitomagnetic quadrupole moment $J_{ij} \rightarrow (1 - \frac{1}{3}\epsilon) J_{ij}$
- No comparable result for $\frac{\mu^2}{M^2}$

Conclusion

- Powerful methods from particle physics for post-Newtonian expansion of compact binaries:
 - Effective field theories
 - Techniques for multiloop calculations
- Latest results:
 - Complete 5PN (near-zone) potential
 - Partial 6PN potential
- Open questions in combination with far zone/tail

Backup

General relativity

General relativity action:

$$S_{\text{GR}}[g^{\mu\nu}] = S_{\text{EH}} + S_{\text{GF}} + S_{\text{matter}}$$

With $\eta^{\mu\nu} = \text{diag}(-1, 1, 1, 1)$, $g = \det(g^{\mu\nu})$:

- Einstein-Hilbert action:

$$S_{\text{EH}} = \frac{1}{16G\pi} \int d^d x \sqrt{-g} R$$

- Harmonic gauge $\partial_\mu \sqrt{-g} g^{\mu\nu} = 0$:

$$S_{\text{GF}} = -\frac{1}{32G\pi} \int d^d x \sqrt{-g} \Gamma_\mu \Gamma^\mu, \quad \Gamma^\mu = g^{\alpha\beta} \Gamma_{\alpha\beta}^\mu$$

- Assume **point-like** matter, no spin:

$$S_{\text{matter}} = -\sum_{a=1}^2 m_a \int d\tau_a$$

General relativity

Post-Newtonian expansion

Expand S_{GR} in $v \sim \sqrt{Gm/r} \ll 1$, e.g.

$$-m_a \int d\tau_a = -m_a \int dt \sqrt{-g_{\mu\nu} \frac{\partial x_a^\mu}{\partial t} \frac{\partial x_a^\nu}{\partial t}} = -m_a \int dt \sqrt{-g_{00}} + \mathcal{O}(v_a)$$

Coupling to **spatial components** of metric **suppressed**

Temporal Kaluza-Klein decomposition [Kol, Smolkin 2010]

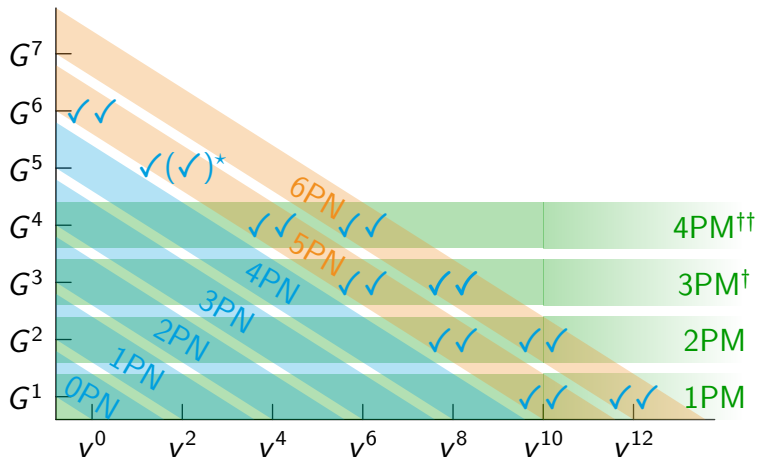
$$g^{\mu\nu} = e^{2\phi} \begin{pmatrix} -1 & A_j \\ A_i & e^{-c_d \phi} (\delta_{ij} + \sigma_{ij}) - A_i A_j \end{pmatrix}, \quad c_d = 2 \frac{d-2}{d-3}$$

Flat spacetime for $\sqrt{Gm/r} \rightarrow 0$:

Expand in $\phi, A_i, \sigma_{ij} \sim \sqrt{Gm/r} \sim v$

Near-zone potential

Cross checks



† [Bern, Cheung, Roiban, Shen, Solon 2019; Cheung Solon 2020; Kälin, Liu, Porto 2020]

†† [Bern, Martinez, Roiban, Ruf, Shen 2021]

* [Foffa, Sturani, Torres Bobadilla 2021]

Far-zone potential

Matching equation for far-zone potential:

$$V_{\text{FZ}} = i \frac{d}{dt} \log \left[\int \mathcal{D}\phi_{\text{rad}} \mathcal{D}A_{\text{rad}} \mathcal{D}\sigma_{\text{rad}} e^{i(S_{\text{mixed}} + S_{\text{radiation}})} \right]$$

Matter-radiation interaction in NRGR:

$$S_{\text{mixed}} = \frac{1}{2} \int d^d x T^{\mu\nu} \delta g_{\mu\nu} + \mathcal{O}(\delta g_{\mu\nu}^2), \quad \delta g_{\mu\nu} = g_{\mu\nu} - \eta_{\mu\nu}$$

$\delta g_{\mu\nu}$ multipole expanded

$\Rightarrow \phi, A_i, \sigma_{ij}$ coupling to multipole moments $E, P_i, L_i, I_{ij}, \dots$

after integration by parts

e.g. [Ross 2012]

Far-zone potential

Matching at 4PN, conservative part:

$$-i \int dt V_{\text{FZ}}^{4\text{PN}} = \begin{array}{c} \begin{array}{ccc} \text{---} & \text{---} & \text{---} \\ | & | & | \\ I & E & I \\ \text{---} & \text{---} & \text{---} \end{array} + \begin{array}{ccc} \text{---} & \text{---} & \text{---} \\ | & | & | \\ I & E & I \\ \text{---} & \text{---} & \text{---} \end{array} + \begin{array}{ccc} \text{---} & \text{---} & \text{---} \\ | & | & | \\ I & E & I \\ \text{---} & \text{---} & \text{---} \end{array} \\ \\ \begin{array}{ccc} \text{---} & \text{---} & \text{---} \\ | & | & | \\ I & E & I \\ \text{---} & \text{---} & \text{---} \end{array} + \begin{array}{ccc} \text{---} & \text{---} & \text{---} \\ | & | & | \\ I & E & I \\ \text{---} & \text{---} & \text{---} \end{array} + \begin{array}{ccc} \text{---} & \text{---} & \text{---} \\ | & | & | \\ I & E & I \\ \text{---} & \text{---} & \text{---} \end{array} \end{array}$$

The diagram illustrates the matching of the far-zone potential at 4PN order. It shows the integral $-i \int dt V_{\text{FZ}}^{4\text{PN}}$ as a sum of six terms. Each term consists of a horizontal line with three points labeled I, E, and I, and a vertical dashed blue line connecting the middle point E to a black dot above it. The terms are distinguished by the color and shape of the arc connecting the two I points: blue dashed, red wavy, and green wavy.

Far-zone potential

Matching at 4PN, conservative part:

$$-i \int dt V_{\text{FZ}}^{4\text{PN}} = \begin{array}{c} \text{---} \overset{\bullet}{\text{---}} \text{---} \\ | \quad | \quad | \\ I \quad E \quad I \end{array} + \begin{array}{c} \text{---} \overset{\bullet}{\text{---}} \text{---} \\ | \quad | \quad | \\ I \quad E \quad I \end{array} + \begin{array}{c} \text{---} \overset{\bullet}{\text{---}} \text{---} \\ | \quad | \quad | \\ I \quad E \quad I \end{array} \\ + \begin{array}{c} \text{---} \overset{\bullet}{\text{---}} \text{---} \\ | \quad | \quad | \\ I \quad E \quad I \end{array} + \begin{array}{c} \text{---} \overset{\bullet}{\text{---}} \text{---} \\ | \quad | \quad | \\ I \quad E \quad I \end{array} + \begin{array}{c} \text{---} \overset{\bullet}{\text{---}} \text{---} \\ | \quad | \quad | \\ I \quad E \quad I \end{array}$$

The equation shows the far-zone potential $-i \int dt V_{\text{FZ}}^{4\text{PN}}$ as a sum of six diagrams. Each diagram consists of a horizontal line with three points labeled I , E , and I from left to right. A vertical dashed blue line connects the middle point E to a black dot above it. A semi-circular arc connects the two I points, passing through the dot. The arcs are colored as follows: the first three diagrams have a dashed blue arc; the fourth has a red wavy arc; the fifth has a red wavy arc on the left and a green wavy arc on the right; the sixth has a green wavy arc.

At 5PN: [Foffa, Sturani 2019–2021]

- Additional multipole moments J_{ij}, O_{ijk}
- More 2-loop diagrams
- 1PN corrections to E, I_{ij} in d dimensions

[Marchand, Henry, Larrouturou, Marsat, Faye, Blanchet 2020]

Classical Hamiltonian

- Combine potentials $V = V_{\text{NZ}} + V_{\text{FZ}}$:

$$L_{\text{PN}}[\vec{x}_a, \vec{v}_a, \vec{a}_a, \vec{x}_a^{(3)}, \dots] = M + T - V$$

- Eliminate higher time derivatives:
 - Total derivatives $L_{\text{PN}} \rightarrow L_{\text{PN}} + \frac{d}{dt} F$
 - Multiple zeroes $L_{\text{PN}} \rightarrow L_{\text{PN}} + F Z_1 Z_2 \dots$
with $\delta(F Z_1 Z_2 \dots) = 0$ at current PN order
 - Coordinate shifts $\vec{x}_a \rightarrow \vec{x}_a + \Delta \vec{x}_a$ with $\Delta \vec{x}_a = \mathcal{O}(1\text{PN})$
- Transform to classical Hamiltonian $H = \vec{p}_a \vec{v}_a - L$ in centre-of-mass frame
- Canonical transformations with generator g for comparisons and simpler expressions

$$H \rightarrow e^{D_g} H, \quad D_g f = \{f, g\}$$